Correlation of Sunspot Numbers and Geomagnetic Indices with Various Climate Change Parameters

S. Adhikari, R. K. Mishra, N. Parajuli, D. P. Adhikari and B. Adhikari

Journal of Nepal Physical Society

Volume 9, Issue 2, December 2023

ISSN: 2392-473X (Print), 2738-9537 (Online)

JNPS, **9** (2): 23-33 (2023)

DOI: https://doi.org/10.3126/jnphyssoc.v9i2.62286

Published by:

Nepal Physical Society
P.O. Box: 2934
Tri-Chandra Campus
Kathmandu, Nepal
Email: nps.editor@gmail.com

JNPS 9 (2): 23-33 (2023)
ISSN: 2392-473X (Print), 2738-9537 (Online)

Research Article *© Nepal Physical Society*
DOI: https://doi.org/10.3126/jnphyssoc.v9i2.62286

Correlation of Sunspot Numbers and Geomagnetic Indices with Various Climate Change Parameters

S. Adhikari[1], R. K. Mishra[2], N. Parajuli[3], D. P. Adhikari[4] and B. Adhikari[2, 3, *]
[1]Central Department of Environmental Science, Tribhuvan University, Kathmandu, Nepal
[2]Department of Physics, St. Xavier's College, Tribhuvan University, Kathmandu, Nepal
[3]Department of Physics, Patan Multiple College, Tribhuvan University, Kathmandu, Nepal
[4]Tri-Chandra Multiple Campus, Tribhuvan University, Kathmandu, Nepal
*Corresponding Email: binod.adhi@gmail.com

Received: *17th September, 2023;* ***Revised:*** *17th October, 2023;* ***Accepted:*** *28th November, 2023*

ABSTRACT

In this paper, a comparative study of climate change parameters with the sunspots number, solar flux, and various geomagnetic indices are presented using statistical methods, cross-correlation analysis and Continuous Wavelet Transform (CWT). From the analysis of 31 years (almost 3 solar cycles) datasets, we observed a positive correlation of sunspot numbers with geomagnetic indices such as AE, Kp, Ap, Dst, and pc. This analysis indicates that variation in sunspot numbers can have a strong influence on the geomagnetic configuration. We also a found perfect positive correlation between CO_2 -CH_4 and CO_2 – TSI, shown with a correlation coefficient of approximately 1 at 0-time lag. The sunspot number shows a high positive correlation with solar flux with a correlation coefficient of 0.95 at 0-time lag indicating that the earth is receiving energy from the sun, which is small but not a negligible fraction of expected global warming. The wavelet analysis carried out on sunspot number (R), Methane emission (CH_4), Carbon dioxide emission (CO_2), Land-Ocean Temperature (LOT), Solar Flux (F10), and, Total Solar Irradiance (TSI) support the evidence of ~11 years of periodicities. Both analyses suggested that the recent climate change is mostly affected by anthropogenic forcing (long-lived greenhouse gases) followed by natural forcing (sunspot number) which cannot be neglected. Thus, the correlation and wavelet analysis suggest that the sun also has a significant role in climate change, and, understanding the role of solar variability is essential to the interpretation of past and prediction of future climate.

Keywords: Sunspots, Geomagnetic Indices, Climate change parameters, Cross-correlation, Continuous Wavelet Transform.

1. INTRODUCTION

Solar Cycle is the periodic variation of the Sun's activity or inactivity for 11-years of time generated by the Solar Magnetic field [1]. Solar Magnetic field created due to the dynamo process is the reason for sunspots, flares, coronal mass ejections, and other types of "magnetic activity" [2]. It might seem implausible that total solar irradiance or "solar constant" which varies with sunspot has an effect on climate change but there is good evidence that solar activity/ sunspot influences the heating and cooling of earth's climate [3]. So that the relation between sunspot (solar cycle) and climate should be understood for future climate prediction and to verify that the solar cycle influences the terrestrial climate [4]. Further research on the topic "solar activity" is necessary for a better understanding of the nature of sunspot number, the most predicted solar activity index [5].

Throughout the solar cycle, the sun goes through a couple of important solar phenomena: solar maxima and solar minima. Sun's total Irradiance between solar maximum and minimum is considered to change by a small amount ~0.1-0.2% but is supposed to contribute to climate change largely [6,7,8] where sunspot maximum cycle 23

has the maximum irradiance [9]. We poorly understood the solar activity cycle [1] and how changes occurring in solar activity act as a forcing mechanism [10]. Cosmic ray reduction can be the major cause of increased solar radiative forcing which greatly magnifies the total solar effect on temperatures [11]. The most obvious direct effect of solar variability on climate is thought to be variations in Total Solar Irradiance (TSI) but the radiative forcing (RF) can have an impact on global mean surface temperature [12].

The climate change has been a major concern of today as it is affecting all the ecosystem and landscapes worldwide including economy, ecology and environment of the region. Increase in modern technological innovations along with economic and social transformation of human society has leads to emission of enormous amount greenhouse gases [13]. Many of these greenhouse gases occur naturally, but human activities are increasing the concentrations of some of them in the atmosphere, in particular, carbon dioxide (CO_2), methane (CH_4), nitrous oxide (N_2O), water vapor (H_2O), and fluorinated gases [14]. Human activities are estimated to have caused approximately 1.0°C of global warming above pre-industrial levels with a likely range of 0.8°C to 1.2°C. Global warming is likely to reach 1.5°C (RCP 8.5) between 2030 and 2052 if it continues to increase at the current rate [14]. This increase in heat has led to the greenhouse effect, resulting in climate change. The main characteristics of climate change are increases in average global temperature (global warming); changes in cloud cover and precipitation particularly over land; melting of ice caps and glaciers and reduced snow cover; and increases in ocean temperatures and ocean acidity due to seawater absorbing heat and carbon dioxide from the atmosphere [15]. Dealing with a controversial topic, the role of the sun in climate change is currently a matter of fierce debate as sun is the ultimate source of energy here on the earth [16]. Therefore, present study focused on comparative study of climate change parameters, Methane (CH4), Carbon dioxide (CO2) and, Land-Ocean Temperature (LOT) with the sunspots number, solar flux (F10.7), Total Solar Irradiance (TSI) and various geomagnetic indices to understand the role of sun in the current climate change.

2. DATASETS AND METHODOLOGY

For this study, we used various space weather parameters such as Solar Flux (F10.7), Sunspot numbers (R), and geomagnetic indices like Kp, Dst, Ap, AE and pc, these indices are numerical values that measure Earth's magnetic field activity. These datasets are taken from the website https://omniweb.gsfc.nasa.gov/. We downloaded the necessary data of various climate change parameters like Carbon dioxide emission (CO_2) from (https://climate.nasa.gov/vital-signs/carbon-dioxide/), Global Land-Ocean Temperature (LOT) from (https://climate.nasa.gov/vital-signs/global-temperature/), Methane emission (CH_4) from (https://www.esrl.noaa.gov/gmd/ccgg/trends_ch4/#global_data) and Total Solar Irradiance (TSI) from (http://spot.colorado.edu/~koppg/TSI/TIM_TSI_Reconstruction.txt).

The statistical tools, Cross-Correlation and Wavelet Analysis are implemented in this work. Correlation is used to determine the degree of association to measure the similarity between different parameters one relative to the other [17, 18, 19, 20].

Wavelet analysis is used to analyze changes in variance where we can determine dominant modes of variability and how these modes vary in time by decomposing time series into time-frequency space [21, 22, 23]. The Continuous Wavelet Transforms (CWT) can provide the time-frequency representation of signal [23, 24]. To extract the information about the behavior of the system, the local time-frequency energy density of a signal can be measured by the wavelet scalogram. The Scalogram is a tool for wavelet analysis which is obtained by taking the squared modulus of the wavelet coefficients [21]. The scalogram is the absolute value of the CWT which is also plotted as a function of time and frequency. In this work, we also use the wavelet power spectrum. The average is taken over all the local wavelet spectra and gives the global wavelet spectrum [21]. The detail mathematical expressions and description of CWT can be found in Torrence & Compo paper [21, 23, 24].

3. RESULTS AND DISCUSSION

Fig. 1. represents the variation of Sunspot Number (R), Methane Emission (CH_4), Carbon dioxide emission (CO_2), Land-Ocean Temperature (LOT), Solar Flux (F10) and Total Solar Irradiance (TSI) as a function of time. The top (first) panel of Fig. 1 represents the sunspot number from 1985-2015. 1986-1989 is the rising phase of the cycle where the number of sunspots increases from minimum value to maximum and became almost constant. The

sunspot numbers were maximum in 1989 and the declining phase began from 1992 until 1996. After that sunspot numbers start to increase and had reached to peak in 2000-2002, whereas declining phase of this period again starts from 2003 to 2008. Sunspot activity after 2009 starts to increase slightly from minimum to maximum and it reaches to peak in the year 2014.

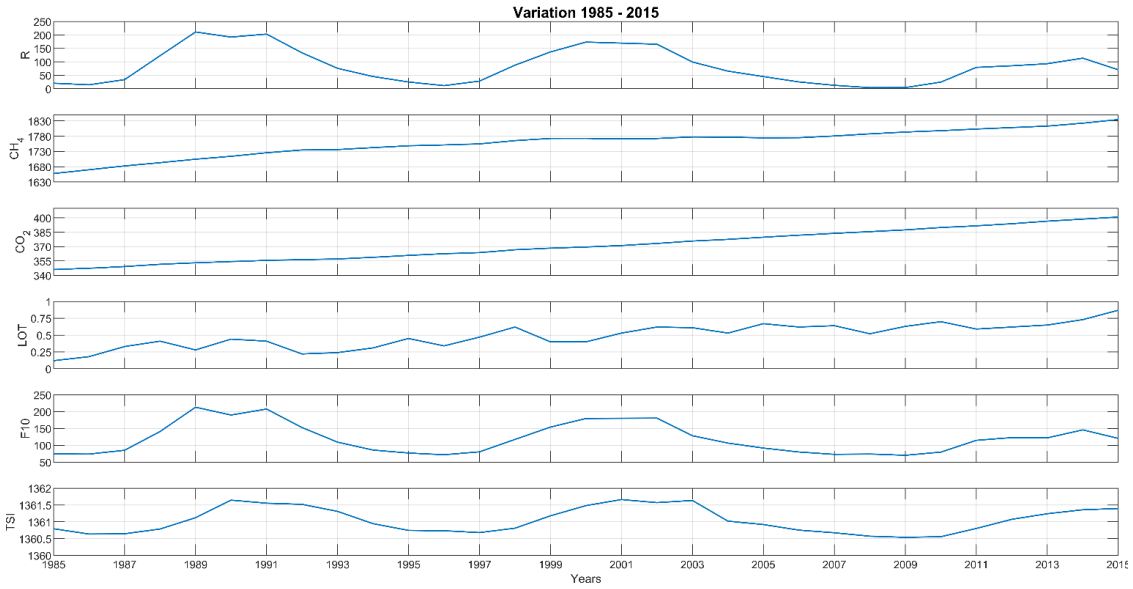

Fig. 1: Variation of Sunspot Number (R), Methane Emission (CH_4), Carbon dioxide Emission (CO_2), Land-Ocean Temperature (LOT), Solar Flux (F10) and Total Solar Irradiance (TSI) from 1985-2015.

The second and third panels of Fig. 1 represent the CH_4 and CO_2 variation from 1985-2015. We observed that the variation of CH_4 and CO_2 are almost similar. This figure shows that CH_4 and CO_2 level have no declining phase, this leads to a conclusion that global CO_2 and CH_4 level is rising so rapidly. We can see that CH_4 level in the year 1985 was about 1655 ppb which has increased and reached a high maximum value of about 1830 ppb in the year 2015. Similarly, in 1985, the level of CO_2 was approximately 345 ppm. Since then, it has increased significantly, peaking at 400 ppm in 2015.

The fourth panel of Fig. 1 represents land-ocean temperature variation from 1985-2015. Overall, increasing pattern of global LOT can be seen. In the year 1985 global temperature was about 0.23^0C. With a little fluctuating pattern, it had reached the highest value of about 0.77^0C in the year 2015. The fifth panel of Fig. 1 represents the variation in solar flux (F10.7) from 1985-2015. The variation on solar flux shows a similar pattern as like Sunspot Numbers. The bottom (sixth) panel of Fig. 1 represents the variation on total solar irradiance (TSI) from 1985-2015. The rising phase of TSI began from 1986-1990 and the peak value observed in the year 1990. Similarly, the declining phase of TSI observed between 1991- 1997. After that with the slight variation, TSI had again reached a maximum value in the year 2001-2003, where the value of TSI was about 1361.7 w/m^2. Another declining phase of TSI was observed between 2005 to 2011. After 2011, TSI again starts to increase and it reached about 1361.4 w/m^2 in the year of 2015.

3.1 Cross-Correlation Analysis

A statistical measure of the relation between two variables as a function of time lag applied to one of them is known as cross correlation. This allows us to check the interaction between two sets of data for each considered scale. It is generally used to measure information between two different time series [24]. The closer positive cross correlation value is 1 [25]. So, we use Pearson's correlation coefficient that ranges from -1 to +1. The portion of curve near +1 depict good linear fit and highest correlation whereas these near 0 depict poor it and less correlation and -1 depict perfect anti correlation [25]. Fig. 2 depicts the results of cross-correlation coefficients of Sunspot Number (R) with different geomagnetic indices for a period of 31 years from 1985 to 2015. The horizontal axis represents the time scale ranging from -31 to 31 years whereas the vertical axis shows the cross-

correlation coefficient scale from 0 to 0.9. It is observed that sunspot number correlates positively with all other geomagnetic indices at a high degree. R – Kp (Red), R – Ap (Purple) and R – AE (Green) relatively overlap with each other throughout the time with maximum correlation coefficients of 0.8551, 0.8747 and 0.8614 respectively, where R is in perfect phase with kp and AE and has a lag of -1 year with ap. In the plot, R shows the least value of positive correlation with pc index ranging to 0.6316 with a very high time lag of -12 years. R – Dst (Yellow) pair shows a positive correlation of 0.8028 where R leads Dst by +3 years.

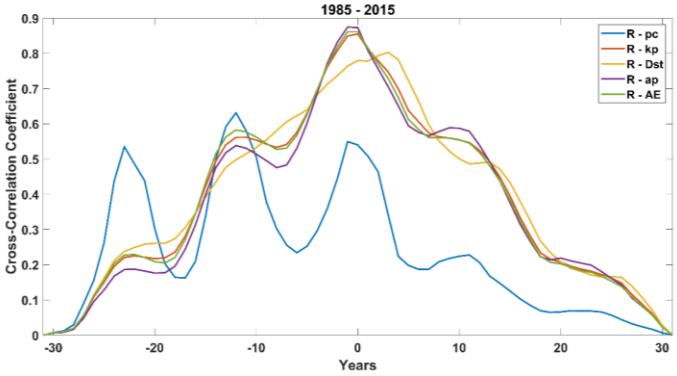

Fig. 2: Cross-correlation of Sunspot Number (R) with pc (Blue), Kp (Red), Dst (Yellow), Ap (Purple) and AE (Green) from 1985- 2015.

Table 1: Correlation coefficients and time lead/lag between Sunspot Number (R) and geomagnetic indices in reference to Fig. 2.

Correlating Parameters	Correlation Coefficient	Time Lead (+) /Lag (-) (years)
R – pc	0.6316	-12
R – Kp	0.8551	0
R – Dst	0.8028	3
R – Ap	0.8747	-1
R – AE	0.8614	0

Different studies have been done to examine the correlation between solar activities and geomagnetic indices. Kilcik et al. [26] show the correlation of r=0.52 with zero-time delay between solar wind speed and Dst for solar cycles 23 and 24 (1996–2014). Le Moue et al. [27] shows Dst is better correlated with sunspot number. Our results also show a high positive correlation with all geomagnetic indices except the polar cap index (pc).

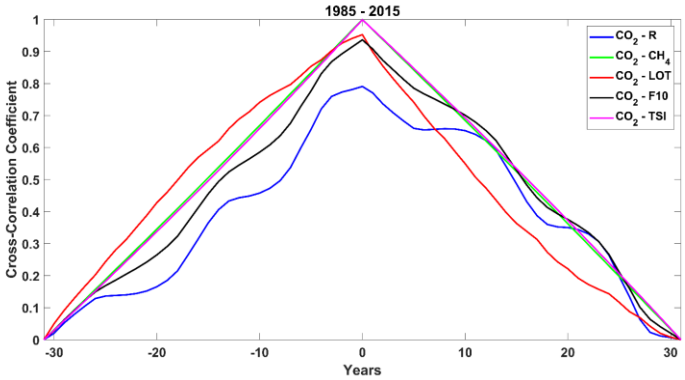

Fig. 3: Cross-correlation of Carbon dioxide emission (CO_2) with other parameters, R (Blue), CH_4 (Green), LOT (Red), F10 (Black) and TSI (Pink) from 1985- 2015.

Table 2: Correlation coefficients and time lead/lag between Carbon dioxide emission (CO_2) and different climate change parameters in reference to Fig. 3.

Correlating Parameters	Correlation Coefficient	Time Lead (+)/Lag (-) (years)
CO_2 – R	0.7908	0
CO_2 – CH_4	0.9998	0
CO_2 – LOT	0.9526	0
CO_2 – F10	0.9364	0
CO_2 - TSI	0.999	0

Fig. 3 depicts the results of cross-correlation coefficients of Carbon dioxide emission (CO_2) with different climate change parameters during a period of 31 years from 1985 to 2015. The horizontal axis represents the time scale ranging from -31 to 31 years whereas the vertical axis shows the cross-correlation coefficient scale from 0 to 1. CO_2 – CH_4 (Green) and CO_2 – TSI (Pink) overlap perfectly throughout the plot and show perfect positive correlation coefficients of 0.9998 and 0.999 with a time lag of 0. Therefore, CO_2 is said to be in perfect phase with CH_4 and TSI. Moreover, it is clear from Table 2 that CO_2 is in perfect phase with all the climate change parameters considered in the study. CO_2 – R (Blue) curve in the plot portrays most fluctuation with the least positive correlation coefficient of 0.7908.

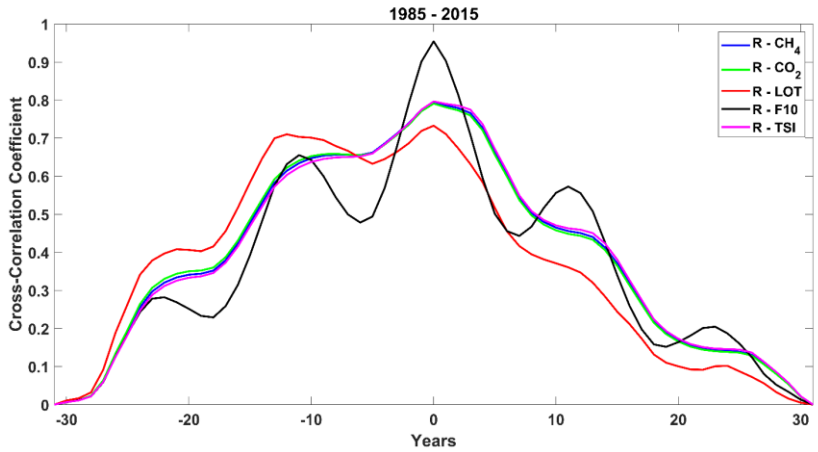

Fig. 4: Cross-correlation of Sunspot Number (R) with other parameters, CH_4 (Blue), CO_2 (Green), LOT (Red), F10 (Black) and TSI (Pink) from 1985- 2015.

Table 3: Correlation coefficients and time lead/lag between Sunspot Number (R) and different climate change parameters in reference to Fig. 4.

Correlating Parameters	Correlation Coefficient	Time Lead (+)/Lag (-) (years)
R – CH_4	0.7952	0
R – CO_2	0.7908	0
R – LOT	0.7328	0
R – F10	0.9544	0
R – TSI	0.7966	0

Fig. 4 depicts the results of cross-correlation coefficients of Sunspot Number (R) with different climate change parameters for a period of 31 years from 1985 to 2015. The horizontal axis represents the time scale ranging from -31 to 31 years whereas the vertical axis shows the cross-correlation

coefficient scale from 0 to 1.R – CH_4 (Blue), R – CO_2 (Green) and R – TSI (Pink) overlap perfectly throughout the plot and reveal positive correlation coefficients of 0.7952, 0.7908 and 0.7966 with a time lag of 0, showing R is in perfect phase with CH_4, CO_2 and TSI. Alike Fig. 3, it is clear from Table 3 that R is in perfect phase with all the climate change parameters considered in the study. However, R shows the highest positive correlation with F10 (Red) and gives a cross-correlation coefficient of 0.9544 at zero-time lag.

Study shows that correlation of sunspot number with local temperature inland Antarctica shows some intermittent periodicities whereas with CO_2 its neither strong nor stable which support the facts solar activity might influence the climate during the past 11,000 years before modern industry [28]. From the study of Scafeta and West (2006) [29,30] the sun has contributed ~ 45-50% between the period of 1900-2000 and 25-35% between the period 1980-2000 for global warming which verifies the importance of sun in climate change but studies suggest that for better understanding of the warming effect after 1970 we need to study the emission of greenhouse gases like CO_2. Souza Echer et al. [31] studied the correlation between global temperature anomaly series and sunspot shows a low correlation of 0.11 in the 11-years solar-cycle and a high correlation of 0.66 in the 22-year band with zero lag. Similarly, from our result, we observed a correlation of 0.7328 in 31-years at zero-time lag.

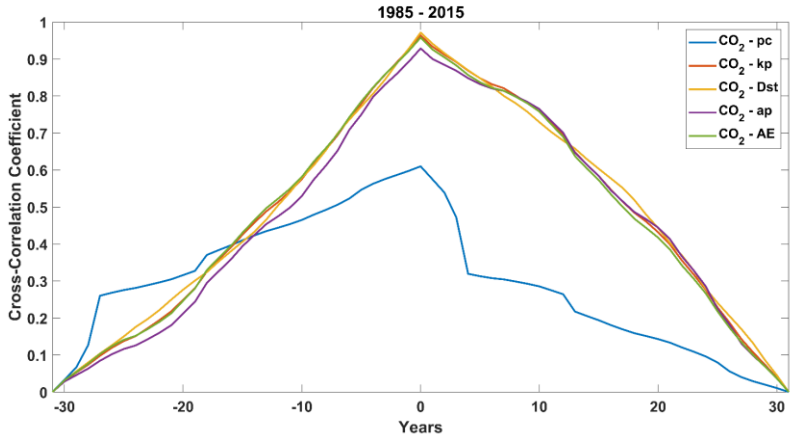

Fig. 5: Cross-correlation of Carbon dioxide (CO_2) with other parameters, pc (Blue), Kp (Red), Dst (Yellow), Ap (Purple) and AE (Green) from 1985- 2015.

Table 4: Correlation coefficients and time lead/lag between Carbon dioxide emission (CO_2) and geomagnetic indices in reference to Fig. 5.

Correlating Parameters	Correlation Coefficient	Time Lead (+)/Lag (-) (years)
CO_2 – pc	0.61	0
CO_2 – Kp	0.9637	0
CO_2 – Dst	0.9715	0
CO_2 – Ap	0.9286	0
CO_2 – AE	0.9579	0

Fig. 5 depicts the results of cross-correlation coefficients of Carbon dioxide emission (CO_2) with different geomagnetic indices during a period of 31 years from 1985 to 2015. The horizontal axis represents the time scale ranging from -31 to 31 years whereas the vertical axis shows the cross-correlation coefficient scale from 0 to 1. CO_2 – Kp (Red), CO_2 – Dst (Yellow), CO_2 – Ap (Purple) and CO_2 – AE (Green) overlaps throughout the plot and reveal positive correlation coefficients of 0.9637, 0.9715, 0.9286 with CO_2 being in perfect phase with kp, Dst, ap and AE. Alike Fig. 3 and 4, it is clear from Table 4 that CO_2 is in perfect phase with all the geomagnetic indices considered in the study. From the fig., it is evaluated that CO_2 has the least positive correlation with pc with a correlation

coefficient of 0.61. From cross-correlation analysis, it has been observed that CO_2 is in perfect phase with all other climate change parameters and geomagnetic indices considered in the study. CO_2 also shows high degree of positive correlation coefficient with all other climate change parameters and geomagnetic indices, with a minimum of 0.61 with pc index and a maximum of 0.998 with CH_4 emission. Sunspot number (R) is in perfect phase with all other climate change parameters and only two geomagnetic indices Kp and AE. Whereas R lags behind pc and Ap index and leads Dst index. Sunspot number also shows high degree of positive correlation coefficients with all other climate change parameters and geomagnetic indices, with a minimum of 0.6316 with pc index and a maximum of 0.9544 with F10.

The pattern and the timing of past climatic conditions are necessary to understand the nature of future climate and to understand the root cause of climate change [32]. Better understanding and interesting results related to the long-term variation of sunspot activity has appeared in the last few years [33]. However, understanding the nature of sun and solar activity and their relationship is still a big challenge in solar physics, since, these activities and radiation output are associated with space weather, biospheric technology and lives on Earth [5]. Even though the continuous rise of solar wind temperature for a long period can have an adverse effect on the global climate, there is a small but noticeable influence of solar activity on the climate on longer time scales particularly on global temperature variation [34, 35].

3.2 Continuous Wavelet Transformation Analysis

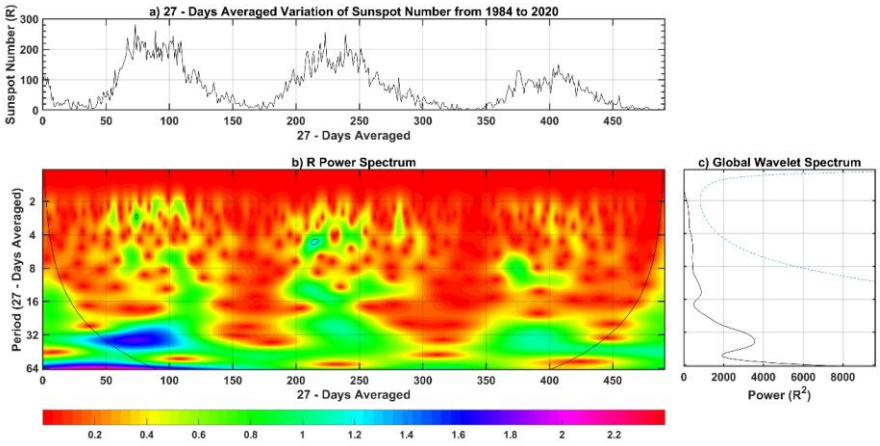

Fig. 6: (a) 27- Days Averaged variations of Sunspot number during 1984 to 2020 (b) Sunspot number Power Spectrum with the color bars selected in square amperes (c) Global spectrum showing main periodicities.

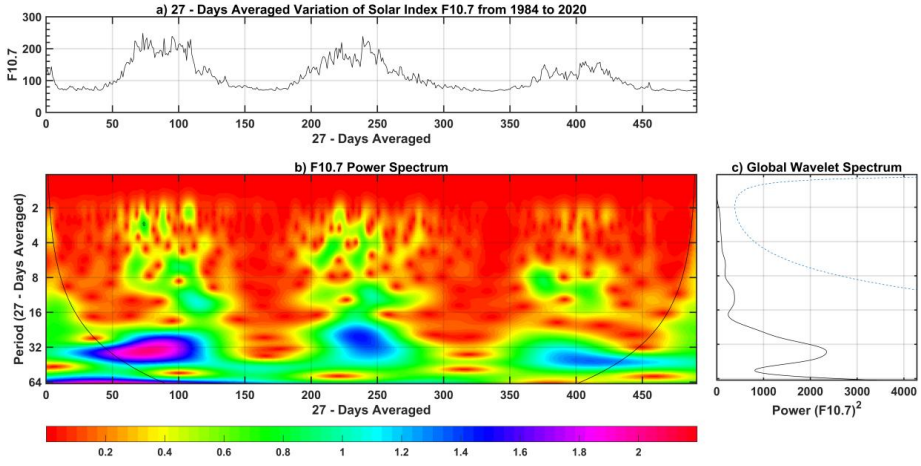

Fig. 7: (a) 27- Days Averaged variations of solar flux during 1984 to 2020 (b)Wavelet scalogram with the color bars selected in square amperes (c) Global spectrum showing main periodicities.

In the wavelet power spectrum, the wavelet power variation is followed by the color code. The higher intensity is observed from red color code and the lower intensity is observed from dark pink color code. In Fig. 6(b), 7(b) the horizontal axis in the scalogram represents the year in 27-averaged days and the vertical axis represents the wavelet spectrum in the form of period (27-days averaged) from 1984 to 2020 for Sunspot and Solar flux. Here in Fig. 6(b) and 7(b) Solar flux and Sunspot Power Spectrum is found between the periods from 16 to 64 for 27-Day averaged and lies inside the cone of influence for respective solar cycles 22, 23 and 24. The Global Wavelet Spectrum have main periodicities ~ 40 and ~ 40, 64 with corresponding energies ~2300 $(F10.7)^2$ and ~3600 R^2, 6000 R^2 for Solar flux and Sunspot respectively. The time series analysis and wavelet analysis indicate solar flux correspondence with sunspot number. Furthermore, this wavelet analysis supports the fact that the sunspot number and Solar flux vary from one cycle to another cycle showing 11-years of periodicities. The wavelet analysis also supports the explanation that SC24 when compared with Sun SC23 and SC22 is less active [36, 37, 38]. The peak of the SC24 is 35% lower than that of SC23 and in the monthly sunspot number record, it is also the fourth largest intercycles drop [39].

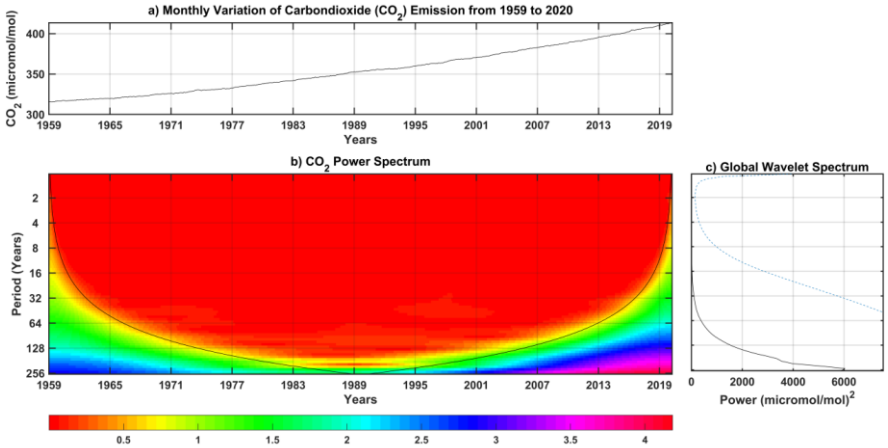

Fig. 8: (a) Monthly variations of Carbon dioxide (CO_2) during 1959 to 2020 (b) CO_2 Power Spectrum with the color bars selected in square amperes (c) Global spectrum showing main periodicities.

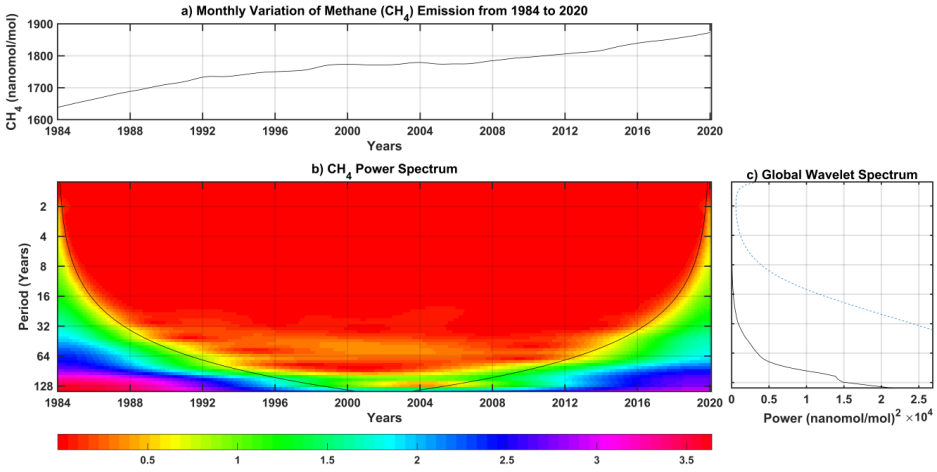

Fig. 9: (a) Monthly variations of Methane (CH_4) during 1984 to 2020 (b) Methane (CH_4) Power Spectrum with the color bars selected in square amperes (c) Global spectrum showing main periodicities.

In Fig. 8(b) and 9(b), the horizontal axis in the scalogram represents the years and the vertical axis represents the wavelet spectrum in the form of period (Years) for different years. In Fig. 8(b) and 9(b), the power area corresponding to CO_2 and CH_4 power spectrum occurs between the period from 128 to 256 and below ~128 respectively but lies outside the cone of influence. In Fig. 8(c) and 9(c),

the Global Wavelet Spectrum have main periodicities ~ 256 and ~ 128 with corresponding energies ~6000 $(micromole/mol)^2$ and ~1.4, $2(micromole/mol)^2 \times 10^4$ for CO_2 and CH_4 respectively. On the time series analysis of CO_2, we observed an increasing linear pattern from the year 1959 to 2020. According to the IPCC, natural source responsible for atmospheric CO_2 is natural disasters like eruption, hurricanes, volcanoes, tsunamis etc. [15, 16] but we can observe the gradual increase from the year 1980 which shows the clear evidence of human influence for the rise of CO_2 concentration in earth's atmosphere [40]. The major cause of increment in the concentration of CO_2 in the earth's atmosphere is the burning of fossil fuels [15, 16] followed by massive deforestation, urban development, and industrialization [40]. CH_4 is released from wetlands as natural emission and livestock farming and agricultural activities like rice production in flooded soils are responsible for anthropogenic emission [41, 42, 16]. Both natural and anthropogenic activities are responsible for CO_2 and CH_4 gas emission. But the gradual increase in the past 50 years shows the influence of anthropogenic contribution.

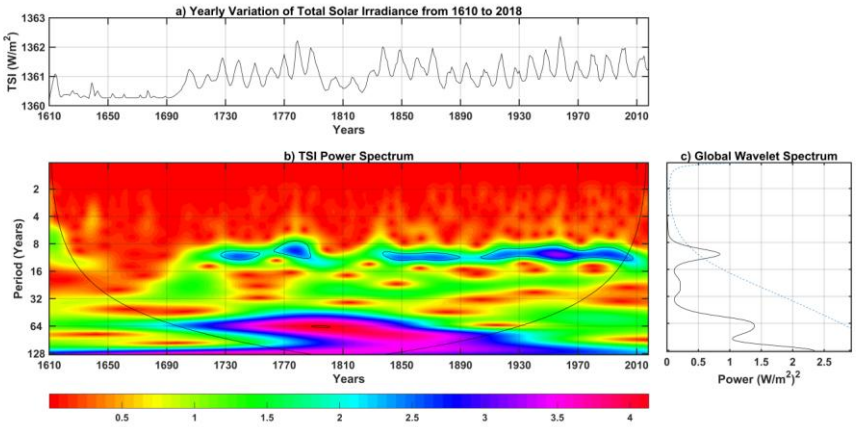

Fig. 10: (a) Yearly variations of TSI from 1959 to 2020 (b) TSI Power Spectrum with the color bars selected in square amperes (c) Global spectrum showing main periodicities.

In Fig. 10(a), the horizontal axis in the scalogram represents the year and the vertical axis represents the wavelet spectrum in the form of period (years) from 1610 to 2018.The TSI Power Spectrum occurs between the periods from 6 to 16 which lie inside the cone of influence at higher frequency regions. Similarly, occurs between the periods from 64 to 128 which lie inside the cone of influence at lower frequency regions. The Global Wavelet Spectrum have main periodicities ~ 9, 64, 128 with corresponding energies ~0.9, 1.4,2.4 (W/m^2) for TSI. Studies have shown that when there are more sunspots, the sun actually become hotter and if there are only few sunspots during solar cycle, earth could probably be cooler [43]. Our results show a lower value of TSI in Maunder minimum (1645-1715), Dalton minimum (1800-1830), Gleissber minimum (1889-1900). The climate cooling during Maunder minimum and Dalton minimum might be due to the lesser solar activities [44]. Solar cycle 17–23 comprising the Modern Maximum [39] where we can also observe Power Spectrum in higher frequencies between the period 8 to 16 which lies inside the cone of influence and shows the maximum sunspot or solar cycle maximum.

In Fig. 11(b), the horizontal axis in the scalogram represents the year and the vertical axis represents the wavelet spectrum in the form of period (Year) from 1880 to 2019. The (Global) LOT Power Spectrum occurs between the period 16 to 32 but lies mostly outside the cone of influence. The Global Wavelet Spectrum of (Global) LOT have main periodicities ~ 10, 24, 32 with corresponding energies ~0.04 C^2, 0.08 C^2, 0.1 C^2. The time series analysis of (Global) LOT variation is always negative (below baseline) but after 1980 the variation is never negative which supports the evidence that (Global) LOT is affected by the rise of GHGs. Our result also explains that the variation in (Global) LOT after 1980 might be more influenced by human activities or the increase of greenhouse gases [16]. Alike Ocean Sea Surface Temperature (SST) [45], in Fig. 11(a) we also witness (Global) LOT vary with the ~11-year cycle similar to that of Solar Cycle.

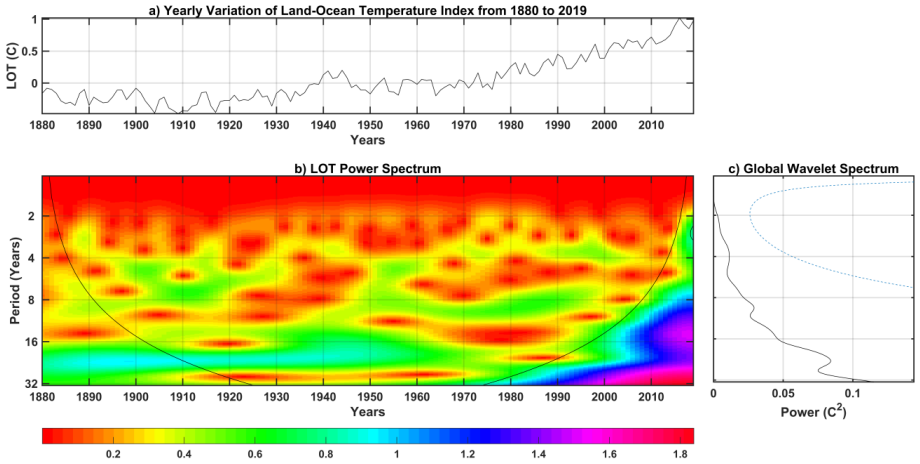

Fig. 11: (a) Yearly variations of Land-Ocean Temperature (LOT) during 1880 to 2020 (b) LOT Power Spectrum with the color bars selected in square amperes (c) Global spectrum showing main periodicities.

CONCLUSION

The solar activity in the sun releases a tremendous amount of energy along with highly accelerated charged particles in the form of solar wind that affects weather on the earth. The present study found positive correlations of CO_2 with other climate change relative parameters like Methane (CH_4), Total Solar Irradiance (TSI), Solar Flux (F10), (Global) Land-Ocean Temperature (LOT) and Sunspot Numbers (R), where CO_2-CH_4 and CO_2-TSI show high positive correlations with correlation coefficient nearly equal to 1 at 0-time lag. Similarly, sunspot numbers show positive correlations with various climate change relative parameters (Methane (CH_4), Total Solar Irradiance (TSI), Solar Flux (F10), Land-Ocean Temperature (LOT) and Carbon dioxide ($CO_{2)}$). This leads to the conclusion that solar brightness has been increasing from previous cycles of sunspot activity to the current one, which indicates that the earth is receiving energy from the sun in increasing order. However, its contribution to global warming is small but not a negligible fraction. To conclude, the sun has a key role in climate change, and understanding the role of solar variability is essential to interpret past climate and prediction of future climate. However further research is essential for the deeper understanding of correlation of sunspot numbers and geomagnetic indices with various climate change parameters. Although this study may suggest potential links between solar activity and climate fluctuations, however a comprehensive study is needed to validate and better understanding of these relationships. In future, extensive further study will be carried out using advanced tools and methodologies for the understanding of relationships between solar activities and terrestrial climate dynamics.

ACKNOWLEDGMENTS

For the study, Solar Flux (F10.7), Sunspot Numbers (R) and geomagnetic indices like Kp, Dst, Ap, AE and pc datasets are taken from the OMNI series from NASA space Physics data facility (https://omniweb.gsfc.nasa.gov/). The necessary data of various climate change parameters like Carbon dioxide emission (CO_2) from (https://climate.nasa.gov/vital-signs/carbon-dioxide/), Global Land-Ocean Temperature (LOT) from (https://climate.nasa.gov/vital-signs/global-temperature/), Methane emission (CH_4) from (https://www.esrl.noaa.gov/gmd/ccgg/trends_ch4/#global_data) and Total Solar Irradiance (TSI) from (http://spot.colorado.edu/~koppg/TSI/TIM_TSI_Reconstruction.txt). The authors would like to thank them.

REFERENCES

[1] Balogh, A.; Hudson, H. S.; Petrovay, K. and Steiger, R. V. Space Sci. Rev., **186**(1-4): 1(2014).

[2] Hoyt, D. V. and Schatten, K. H. *The Role of the Sun in Climate Change* (Oxford University Press (1997).

[3] Haigh, J. D.; Living, Rev. Sol. Phys., **4:** 2 (2007).

[4] Arora, K.; Chandrasekhar, N. P.; Nagarajan, N. and Singh, A. JAtmos Sol-Terr Phy, **114:** 19 (2017).

[5] Chattopadhyay, G. and Chattopadhyay, S. Eur. Phys. J. Plus, **127**: 43 (2012).

[6] Eddy, J. A. Clim. Change, **1:** 173 (1977).

[7] Friis-Christensen, E. and Lassen, K. Science, **254** (5032): 698(1991).

[8] Willson, R. C. and Hudson, H. S. Nature, **351**: 42 (1991).

[9] Rind, D. Science, **296** (5568): 673 (2002).

[10] Engels, S. and Geel, B.V. J. Space Weather Space Clim., **2** (A09): 9 (2012).

[11] D'Aleo, J. S. *Solar Changes and the Climate* (American Meteorological Society, Hudson, NH, United States, p. 263 (2016).

[12] Gray, L. J.; Beer, J.; Geller, M.; Haigh, J. D.; Lockwood, M.; Matthes, K. and White, W. Rev. Geophys., **48**: RG4001(2010).

[13] Schild, A. The mountain perspective as an emerging element in the international development agenda. *ICIMOD Newsletter*, **53**: 5-8 (2007).

[14] IPCC. Summary for Policymakers: Climate Change 2022_ Impacts, Adaptation and Vulnerability_Working Group II contribution to the Sixth Assessment Report of the Intergovernamental Panel on Climate Change. In *Working Group II contribution to the Sixth Assessment Report of the Intergovernamental Panel on Climate Change* (2022).

[15] IPCC, Climate Change 2007: Synthesis Report. Contribution of Working Groups I, II and III to the Fourth Assessment Report of the Intergovernmental Panel on Climate Change (2007).

[16] Darkwah, W. K.; Odum, B.; Addae, M.; Desmond, K.; Benjamin, K. D.; Ewurabena, O.; Theophilus, A. and Beryl, B. Journal of Scientific Research and Reports, **17**: 1 (2018).

[17] Asuero, A.; Sayago, A. G. and González, A. G. Crit Rev Anal Chem, **36** (1): 41 (2006).

[18] Galton, F. *Proceedings of the Royal Society of London* (Royal Society, London, December 5, 1888), p. 135.

[19] Adhikari, B. ; Khatiwada, R. and Chapagain, N. P. Journal of Nepal Physical Society, **4**: 119 (2017).

[20] Adhikari, B.; Dahal, S. and Chapagain, N. P. Earth Space Sci., **4** (5): 257 (2017).

[21] Torrence, C. and Compo, G. P. Bull. Amer. Meteor. Soc., **79**: 61 (1998).

[22] Adhikari, B. and Chapagain, N. P. Journal of Nepal Physical Society, **3**(1): 6 (2015).

[23] Gautam, S. P.; Silwal, A.; Baral, B.; Subedi, S.; Lamichhane, N., Chapagain, N. P. & Adhikari, B. Influence of the rainfall and temperature oscillation on air quality in Kathmandu valley: The wavelet analysis. *Environmental Engineering Research*, **28**(6): 0-3 (2023).

[24] Adhikari, B.; Baruwal, P. and Chapagain, N. P. Earth Space Sci, **4**(1): 2 (2017).

[25] Katz, R. W. Use of cross correlations in the search for teleconnections. *Journal of Climatology*, **8**(3): 241–253 (1988).

[26] Kilcik, A.; Yiğit, E.; Yurchyshyn, V.; Ozguc, A.; Rozelot, J. P. Sun and Geosphere, **12**(1): 31 (2017).

[27] Le Mouel, J.; Blanter, E.; Shnirman, M. and Courtillot, V. J Geophy Res-Space, **117**: A09103(2012).

[28] Zhao, X. H. and Feng, X. S. JAtmos Sol-Terr Phy, **122**: 26 (2015).

[29] Scafetta, N. and West, B. J. Geophys. Res. Lett., **33** (5): L05708 (2006).

[30] Li, Z.; Yue, J.; Xiang, Y.; Chen, J.; Bian, Y. and Chen, H. Adv Meteorol, **2018:** 1 (2018).

[31] Souza Echer, M. P.; Echer, E.; Nordemann, D. J. R. and Rigozo, N. R. JAtmos Sol-Terr Phy, **71**(1): 41 (2009).

[32] Vandenberghe, J.; Coope, R. and Kasse, K. J. Quat Sci, **13**(5): 361(1998).

[33] Usoskin, I. G. & Mursula, K. Sol Phys, **218**(1/2): 319 (2003).

[34] Lockwood, M.; Rouillard, A. P. and Finch, I. D. Astrophys J., **700**(2): 937 (2009).

[35] Weber, W. Annalen Der Physik, **19** (6): 372 (2010).

[36] Ahluwalia, H. S. and Jackiewicz, J. Adv in Space Res, **50**(6): 662 (2012).

[37] Svalgaard, L.; Cliver, E. W. and Kamide, Y. Geophys. Res. Lett., **32**: L01104 (2005).

[38] Schatten, K. H.; Geophys. Res. Lett., **32**: L21106 (2005).

[39] Petrovay, K. Living Rev Sol Phys, **17**: 2 (2020).

[40] Mgbemene, C. A.; Nnaji, C. C. and Chekwubechukwu, N. J. Environ. Sci. Technol., **9**(4): 301 (2016).

[41] Leip, A.; Weiss, F.; Wassenaar, T.; Perez, I.; Fellmann, T.; Loudjani, P.; Tubiello, F.; Grandgirard, D.; Monni, S. and Biala, K. Evaluation of the livestock sector's contribution to the EU greenhouse gas emissions (GGELS) - final report, 2010.

[42] Ruddiman, W. F. and Thomson, J. S. Quat. **Sci**. Rev., **20**(18): 1769 (2001).

[43] Eddy, J. The Maunder Minimum Science **192**: 1189-1202 (1976).

[44] Tapping, K. F.; Boteler, D.; Charbonneau, P.; Crouch, A.; Manson, A. and Paquette, H. Sol. Phys., **246**: 309 (2007).

[45] Shaviv, N. J. J. Geophys. Res. **113**: A11101 (2008).